Supplementary Information

Remotely Controlled Chemomagnetic Modulation of Targeted Neural Circuits

Siyuan Rao, Ritchie Chen, Ava A. LaRocca, Michael G. Christiansen, Alexander W. Senko, Cindy H. Shi, Po-Han Chiang, Georgios Varnavides, Jian Xue, Yang Zhou, Seongjun Park, Ruihua Ding, Junsang Moon, Guoping Feng, and Polina Anikeeva*

*All questions and requests for samples should be addressed to: anikeeva@mit.edu

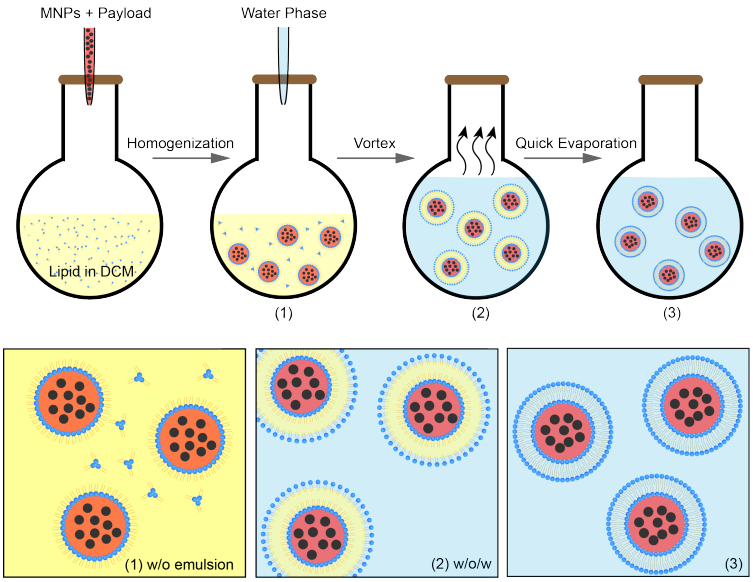

Fig. S1. Magnetoliposome synthesis via double-emulsion method. The aqueous solution of MNPs and payload was added into the mixtures of lipids that were dissolved in an organic solvent (dichloromethane, DCM). After homogenization, large volume of the second water phase was added, followed by vortex homogenization and rapid evaporation.

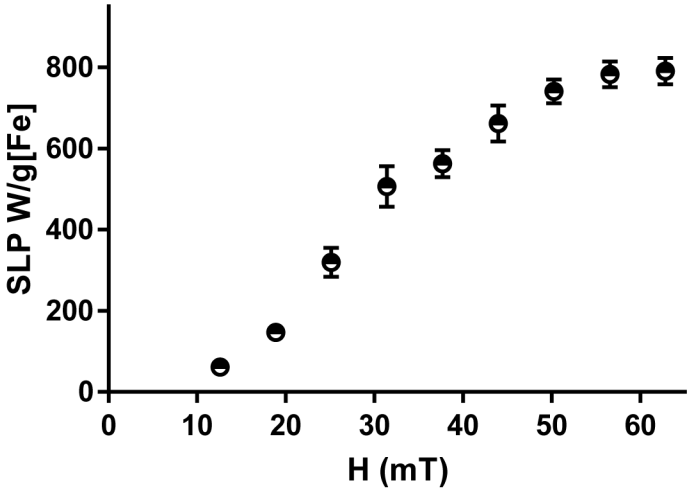

Fig. S2. Specific loss of power (SLP) of iron oxide nanoparticles. The measurements were conducted under AMF with frequency f=150 kHz and amplitude H=12.6, 18.9, 25.1, 31.4, 37.7, 44.0, 50.3, 56.6, and 62.8 mT (10, 15, 20, 25, 30, 35, 40, 45, and 50 kA/m, error bars represent standard deviation, s.d., n=3 independent experiments). The SLP increases with the increasing AMF amplitude and then reaches saturation at fields approaching the coercive field of the particles. The data were acquired with a custom calorimetry setup equipped with an AMF coil driven by a resonant circuit reported in our previous studies1-3.

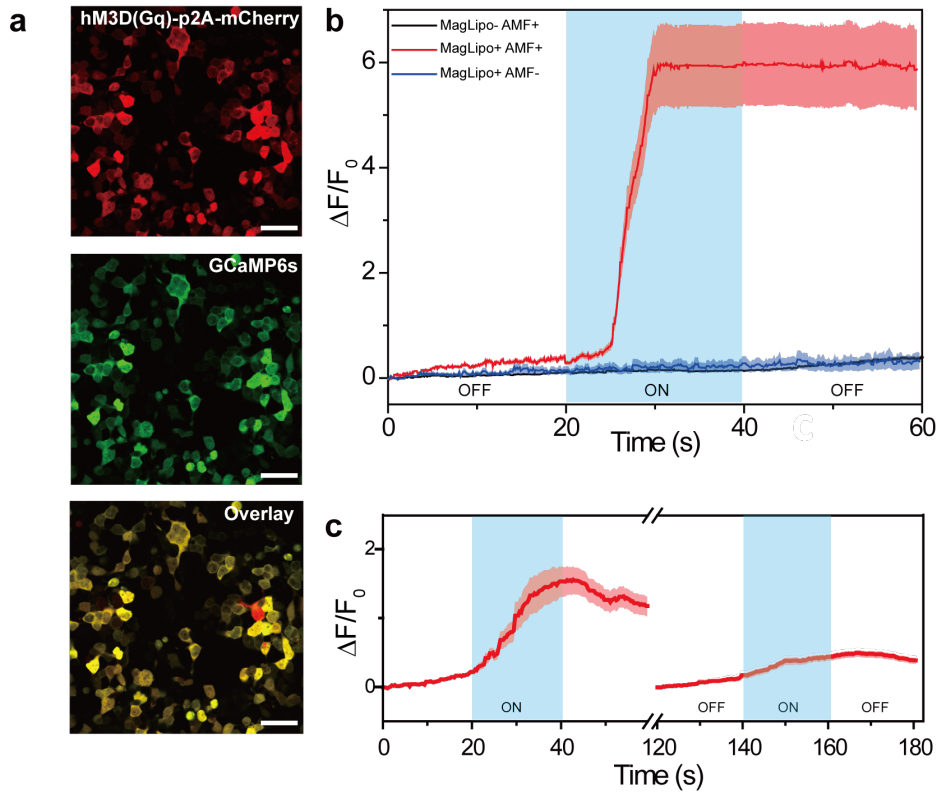

Fig. S3. ***In vitro*** **magnetic stimulation on human embryonic kidney (HEK) cells**. **a**, Confocal microscope images of HEK293 cells expressing *CamKIIa::hM3D(Gq)-p2A-mCherry* and *CMV::GCaMP6s*. The experiment was repeated three times independently with similar results. Scale bar: 50 µm. **b**, Normalized GCaMP6s fluorescence ($\Delta F/F_0$) for cells incubated or not incubated with magnetoliposomes loaded with CNO in the presence or absence of AMF stimulation. **c**, Multiple increases in GCaMP6s fluorescence were observed upon repeated exposure to AMF. AMF conditions: amplitude H_0=45±2 mT, frequency f=150 kHz, duration 20 s. The blue shaded areas represent AMF stimuli. Solid lines: mean, shaded areas: standard error of the mean (s.e.m). For each condition, n=50 cells.

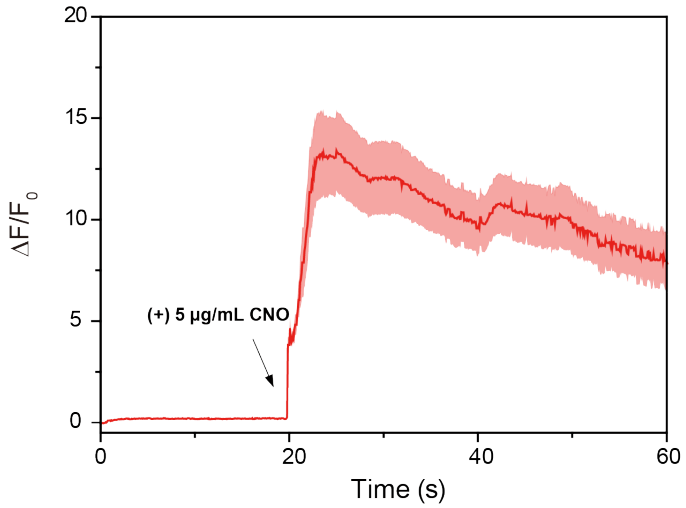

Fig. S4. Corroboration of the functional expression of hM3D(Gq) in primary hippocampal neurons co-transfected with GCaMP6s. Normalized GCaMP6s fluorescence ($\Delta F/F_0$) increase in response to direct application of the CNO solution (5 µg/ml) to the neuronal culture. Solid lines: mean, shaded areas: s.e.m., n=50 neurons.

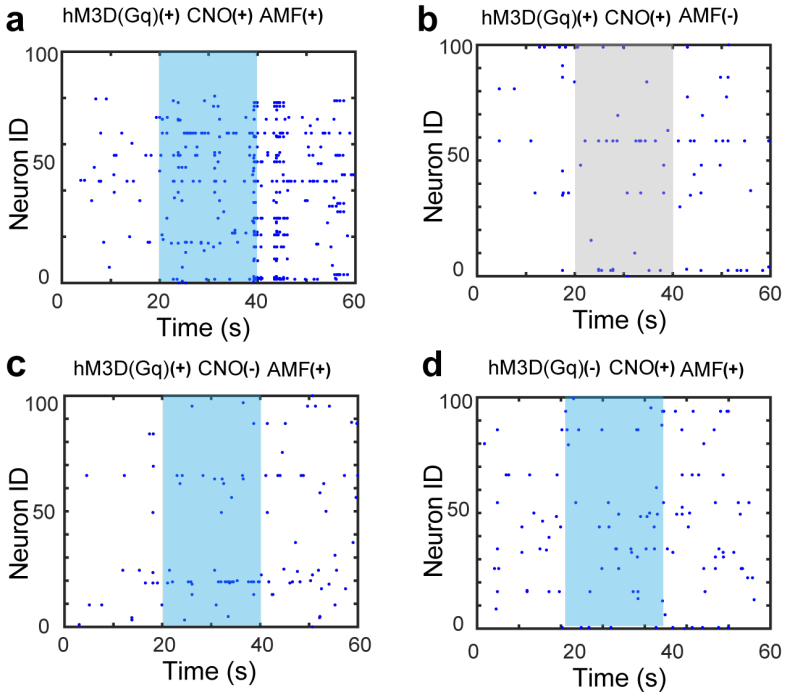

Fig. S5. Raster plots of GCaMP6s fluorescence spikes for 100 randomly automatically selected hippocampal neurons in different test conditions. Calcium spikes were counted as crossings of 7 standard deviations (7σ) threshold from the baseline fluorescence noise using a previously reported algorithm4. The blue area represents the 20 s epochs when AMF (f=150 kHz, H_0 = 45±2 mT) is on. The grey area represents the 20 s epochs without AMF stimulation.

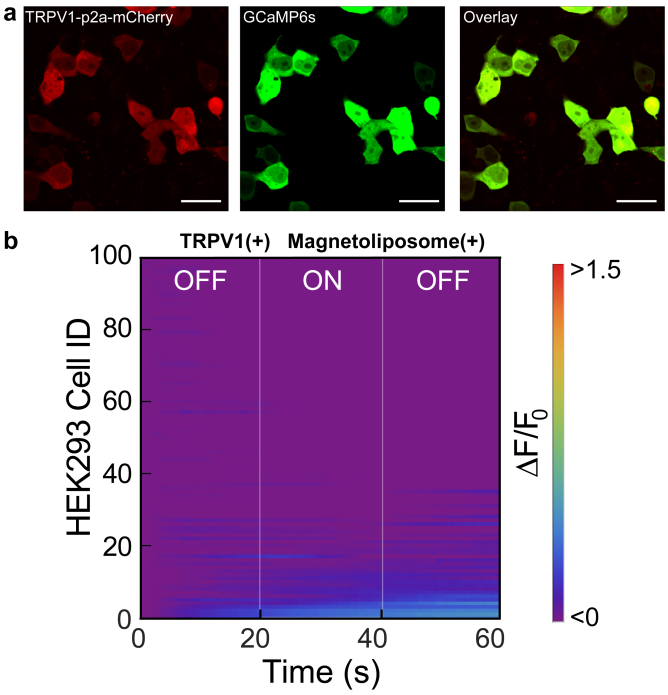

Fig. S6. Assessment of magnetoliposome heating effects *in vitro*. a, Confocal microscope images of human embryonic kidney (HEK293) cells expressing heat-sensitive transient receptor potential cation channel subfamily V member 1 (TRPV1) (*CamKIIα::TRPV1-p2A-mCherry*) and fluorescent calcium indicator, GCaMP6s (*CMV::GCaMP6s*). The experiment was repeated three times independently with similar results. Scale bar: 50 μm. **b**, The heat map of normalized GCaMP6s fluorescence intensity of 100 automatically selected cells with magnetoliposomes. No TRPV1 activation was observed consistent with negligible changes in solution temperature (Fig. 1d). ON: AMF is turned on. OFF: AMF is turned off. AMF conditions: H_0=45±2 mT, f=150 kHz, 20 s.

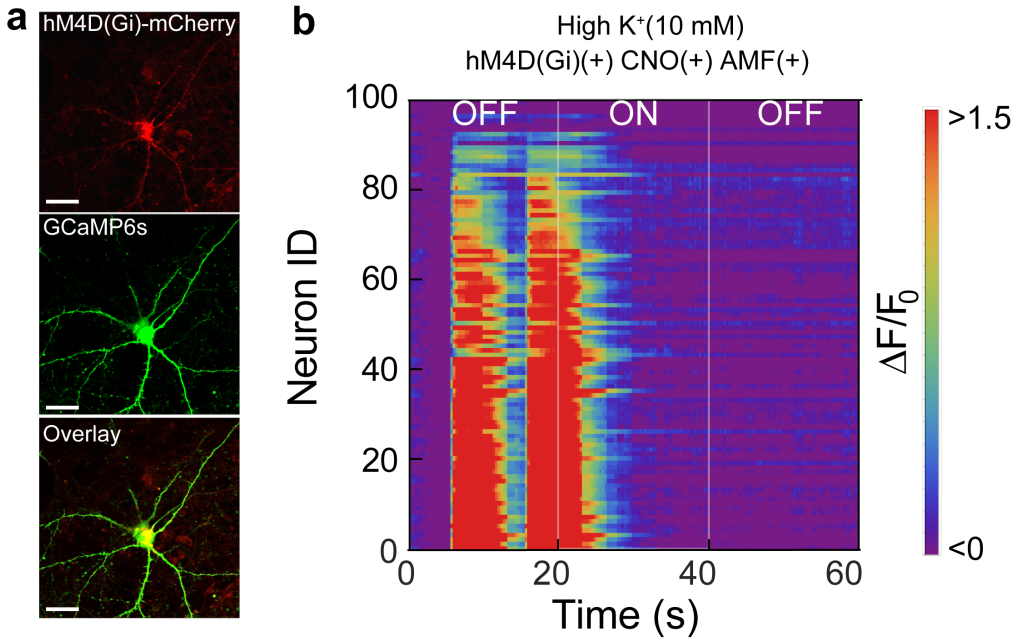

Fig. S7. Chemomagnetic inhibition *in vitro*. a, Confocal images of the primary hippocampal neurons expressing *hSyn::hM4D(Gi)-mCherry* and *hSyn-GCaMP6s*. The experiment was repeated three times independently with similar results. Scale bar: 25 μm. **b**, The heat map of normalized GCaMP6s fluorescence intensity of 100 automatically selected neurons in high potassium (K^+) Tyrode solution with CNO loaded magnetoliposomes. High K^+ Tyrode was used to increase background firing in a neuronal network[5,6]. ON: AMF is turned on. OFF: AMF is turned off. AMF conditions: H_0=45±2 mT, f=150 kHz, 20 s.

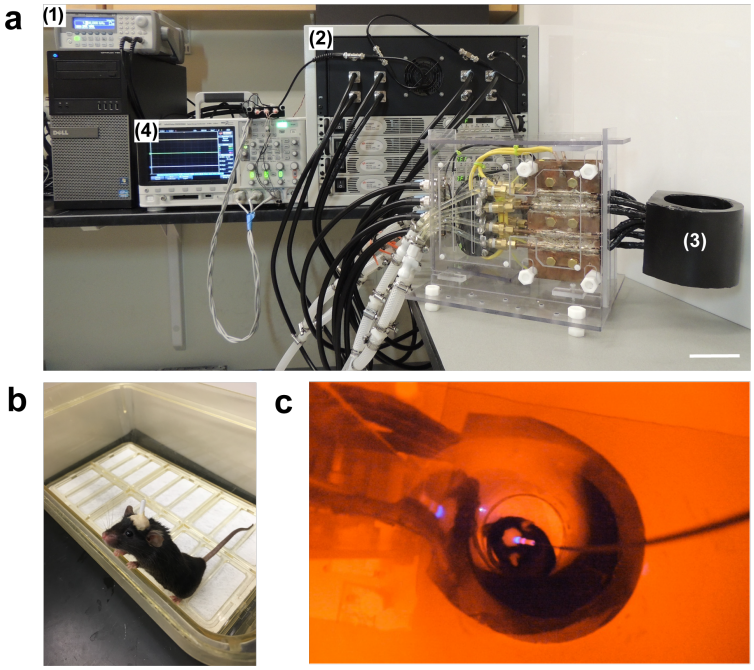

Fig. S8. Fibre photometry apparatus integrated with the AMF stimulation coil and driving electronics. a, The AMF stimulation setup consists of a function generator (1), a custom-designed inverter driven by four direct current (DC) voltage sources (2), a resonant tank circuit including the AMF coil (3) and a capacitor tailored to a desired resonance frequency, and an oscilloscope (4). Scale bar: 5 cm. **b**, A photograph of a mouse implanted with an optical fiber ferrule. **c**, A photograph of a mouse moving with the AMF coil during dynamic photometric recording of GCaMP6s fluorescence.

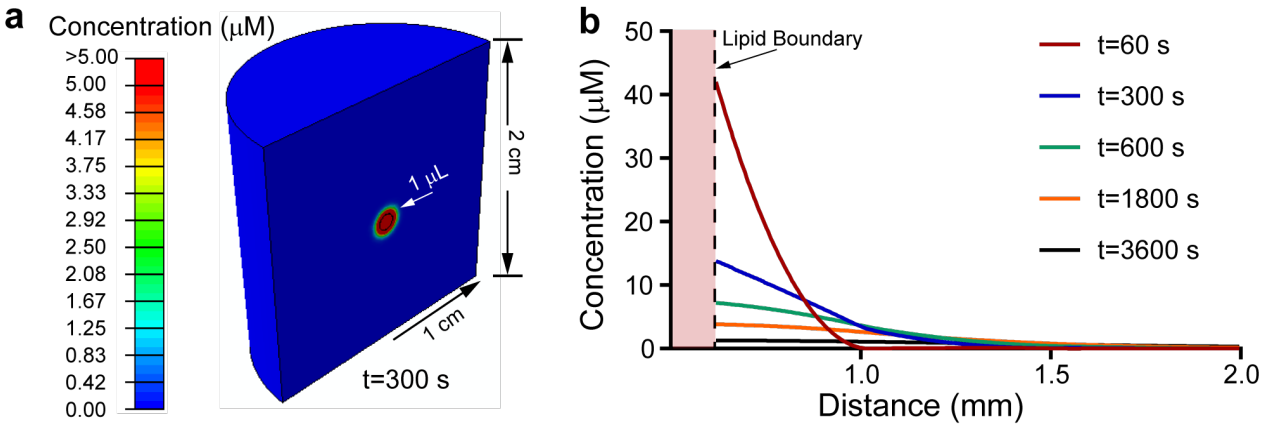

Fig. S9. A model of CNO diffusion in the brain following AMF exposure. a, the Abaqus model was used to calculate the CNO distribution around the magnetoliposome injection site within the brain tissue. The mass diffusion behaviour was described by Fick's law within the model. **b**, the CNO distribution curves from the centre of the magnetoliposome injection site following diffusion times ranging from 60 s to 3600 s. The CNO release is calculated with 40-second AMF stimulation. The equation and corresponding physical parameters of the model are provided in the Supplementary Table S1.

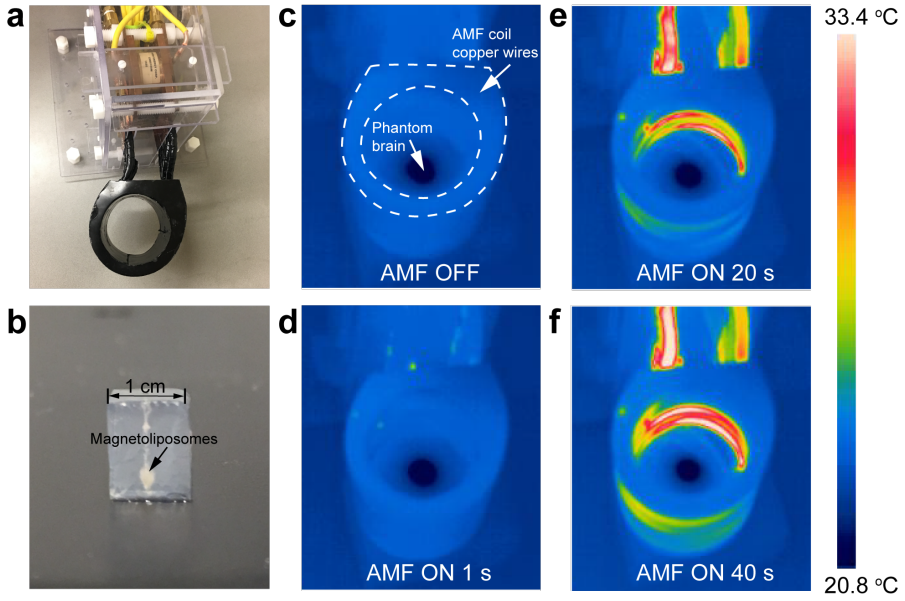

Fig. S10. Assessment of magnetoliposome bulk heating effects. a-b, Photographs of the AMF coil and a phantom brain (0.6% agarose gel) with 1 μL of magnetoliposome injected inside. **c-f,** Photographs by an infrared camera of the phantom brain with magnetoliposomes inside of the AMF coil when AMF is OFF, and applied 1 second, 20 and 40 seconds. The colour bar indicates the temperature. During the AMF exposure time, the magnetoliposomes did not induce bulk heating effects in the phantom brain consistent with thermometry in solutions of identical concentration (Fig. 1d).

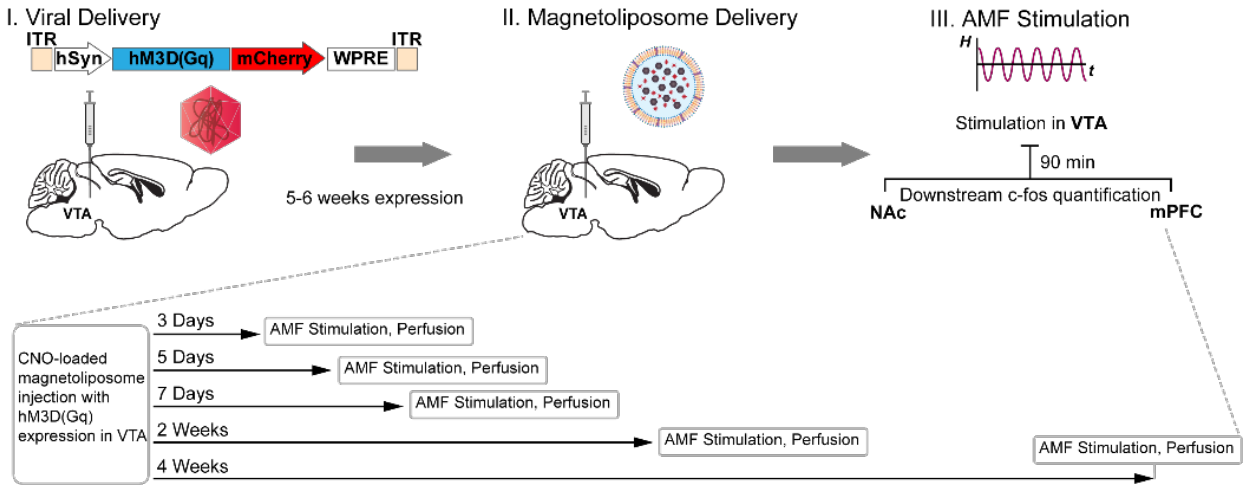

Fig. S11. The experimental timeline for the viral gene delivery, magnetoliposome injection, AMF stimulation and c-fos quantification at a series of time point. All the mice were exposed to AMF (AMF^{+}), injected with CNO-loaded magnetoliposomes (CNO^{+}) and were expressing hM3D(Gq) ($hM3D(Gq)^{+}$) in the VTA. All c-fos quantification experiments were conducted in anesthetized mice.

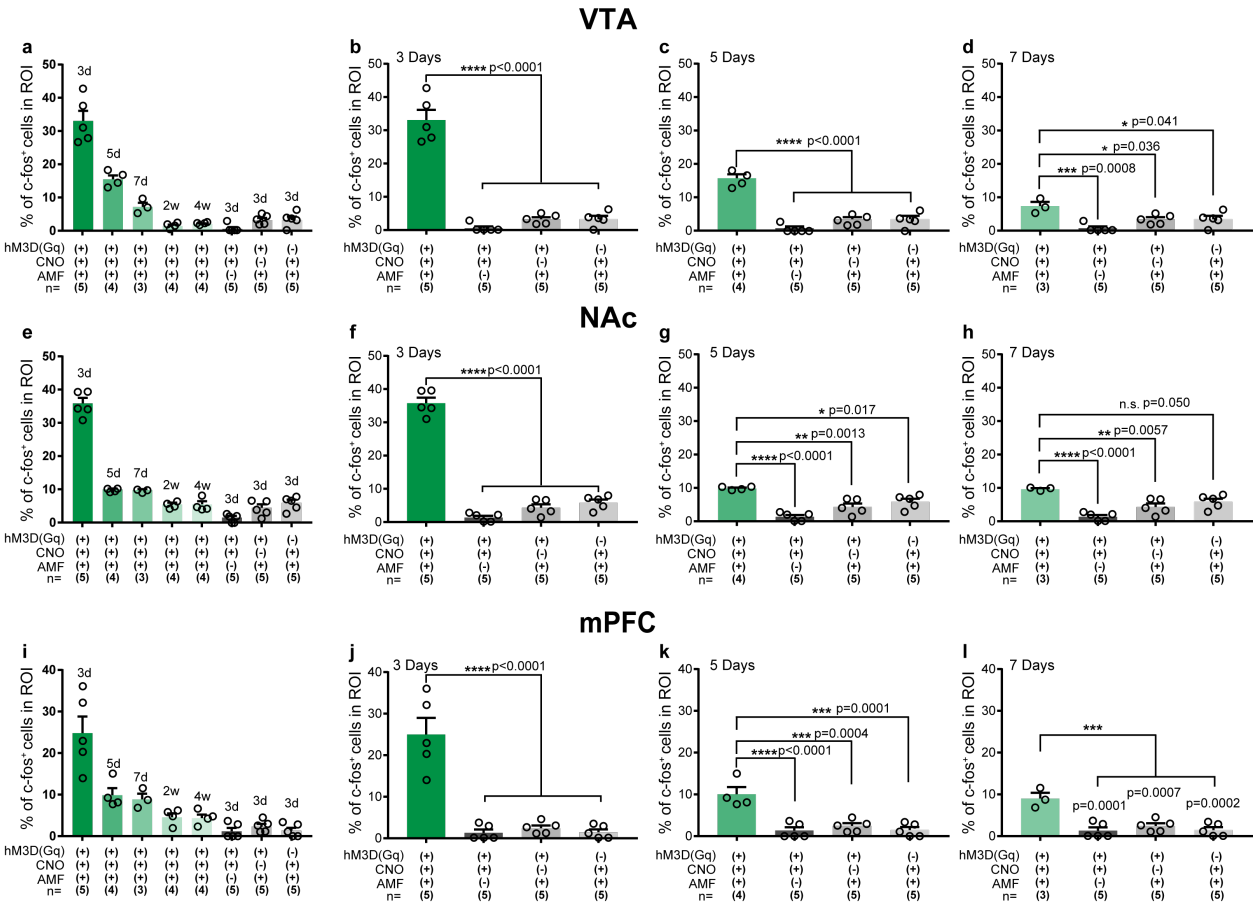

Fig. S12. c-Fos quantification at a series of time points up to 4 weeks. Statistical comparison of c-fos expression level (mean ± s.e.m.) when AMF stimulation (AMF^+) was applied 3 days, 5 days and 7 days following CNO-loaded magnetoliposome (CNO^+) injection into the VTA of mice expressing hM3D(Gq) ($hM3D(Gq)^+$). Increased c-fos expression in the VTA and its projection targets, NAc and mPFC, in response to AMF stimulation is observed up to 7 days following magnetoliposome delivery, as confirmed by one-way ANOVA and Turkey's multiple comparisons test (VTA 3 Days $F_{3,16} = 86.29$, 5 Days $F_{3,15} = 56.72$, 7 Days $F_{3,14} = 8.84$, NAc $F_{3,16} = 207.6$, 5 Days $F_{3,15} = 18.37$, 7 Days $F_{3,14} = 14.13$, mPFC $F_{3,16} = 30.97$, 5 Days $F_{3,15} = 16.73$, 7 Days $F_{3,14} = 15.04$, n.s. $p \geq 0.05$, * $0.01 \leq p < 0.05$, ** $0.001 \leq p < 0.01$, *** $0.0001 \leq p < 0.001$, **** $p < 0.0001$), *n* represents the number of subjects.

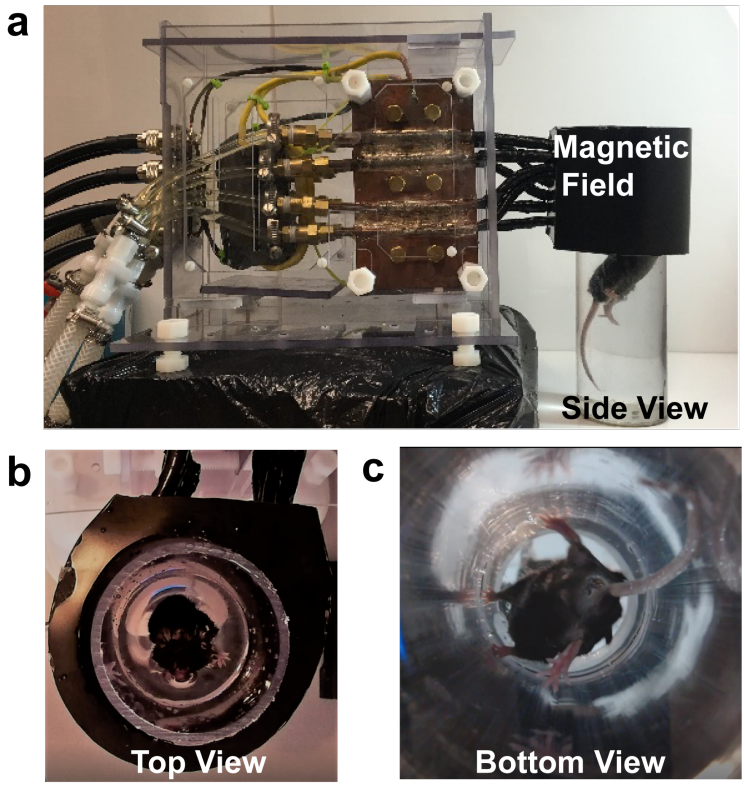

Fig. S13 Forced swimming test (FST) setup integrated with the AMF stimulation coil. Side view (**a**), top view (**b**), and bottom view (**c**) of a mouse undergoing FST during AMF stimulation. The mouse head was positioned inside of the stimulation volume with the uniform AMF amplitude by adjusting the swimming tank water level.

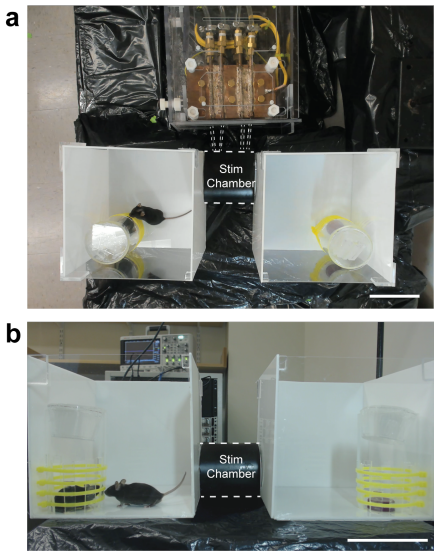

Fig. S14 Social preference setup integrated with the magnetic stimulation coil. **a**, Top view of the experimental arena. The magnetic coil surrounded the stimulation chamber connecting to the social (with a stranger mouse) and the neutral (with a new object) chambers. Following AMF exposure, the stimulation chamber served as a passage between the two test chambers and allowed the mice to freely explore the entire arena. Scale bar: 10 cm. **b**, Side view of the social preference arena. Scale bar: 10 cm.

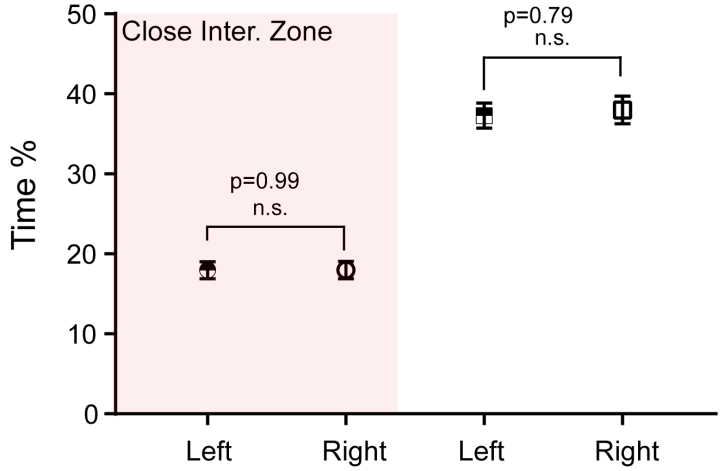

Fig. S15. Place preference control tests. Percentage of time spent in each test chamber on Day 0 in the absence of novel objects or social subjects. The pink area corresponds to the percentage of time spent in the close interaction zone (radial area, 90% of the arena length/width). No significant differences (n.s. $p \geq 0.05$) were found between the chambers (mean ± s.e.m.), n=39 mice, two-tailed paired t-test.

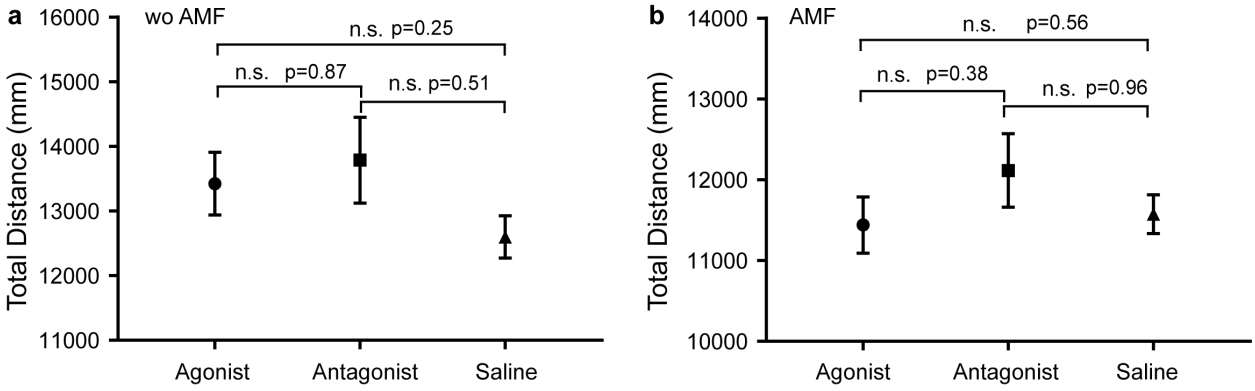

Fig. S16 Locomotor control tests for WT mice injected with magnetoliposomes carrying different payloads. a, The total distance traveled within the entire arena by mice injected with magnetoliposomes loaded with either agonist (SKF-38393), antagonist (SCH-23390), or saline without AMF stimulation. No significant differences were found between the groups (error bars represent mean ± s.e.m., one-way ANOVA, agonist n=30 trials, antagonist n=30 trials, saline n=27 trials, $F_{2, 84}$ = 1.32, n.s. p≥0.05). **b**, The total distance traveled within the entire arena by the test mice injected with magnetoliposomes loaded with either agonist (SKF-38393), antagonist (SCH-23390), or saline following AMF stimulation. No significant differences were found between the groups (mean ± s.e.m., one-way ANOVA, agonist n=30 trials, antagonist n=30 trials, saline n=27 trials, $F_{2, 84}$ =0.9803, n.s. p≥0.05).

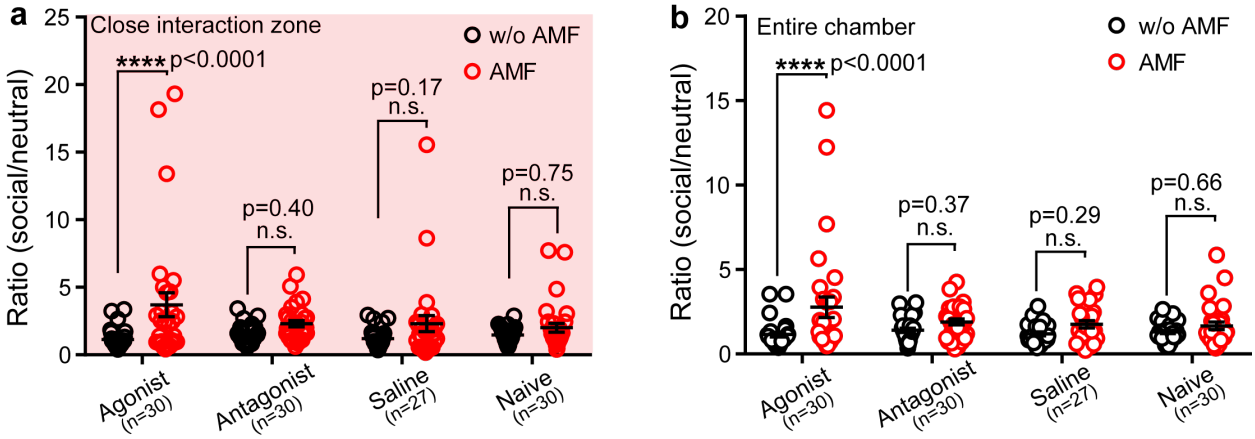

Fig. S17. The ratio of time spent in the social interaction chamber to the neutral object chamber is compared for mice subjected to AMF across all individual trials. The group with agonist-loaded magnetoliposomes exhibits enhanced social preference following exposure to AMF as compared to the groups injected with antagonist or saline-loaded magnetoliposomes and to the naive strain- and age-matched mice without any surgeries (mean ± s.e.m., two-way repeated measures ANOVA and Sidak's multiple comparisons test, close interaction $F_{3, 113}$= 3.053, entire chamber $F_{3,113}$=3.547, n.s. p≥0.05, **** p< 0.0001). *n* represents number of trials.

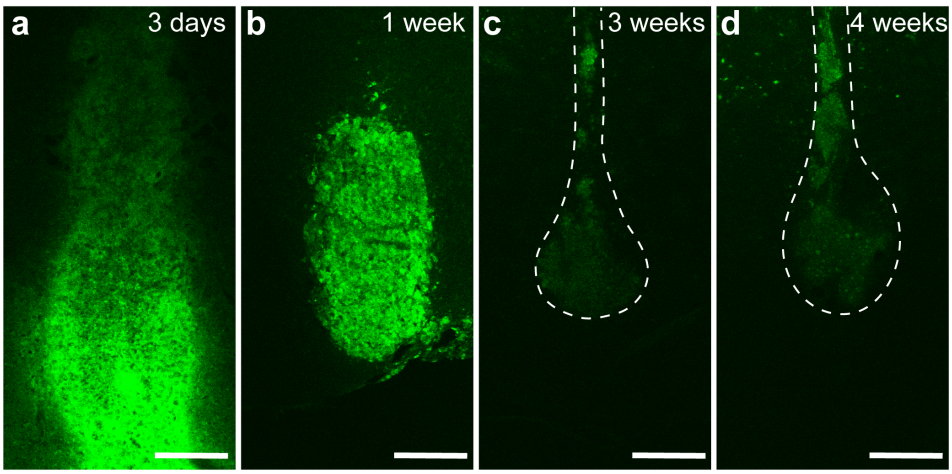

Fig. S18. ***In vivo*** **stability assessment of magnetoliposomes.** Alexa 488 dye-loaded magnetoliposomes were injected into the mouse VTA according to the procedures identical to those used for the CNO or neuromodulator-loaded magnetoliposomes. 40 μm thick brain slices were prepared using a cryo-vibratome 3 days (**a**), 1 week (**b**), 3 weeks (**c**) and 4 weeks (**d**) following injection. **a-d**, Confocal images of the dye-loaded magnetoliposome injection sites. The experiment was repeated three times independently with similar results. Scale bar: 200 μm.

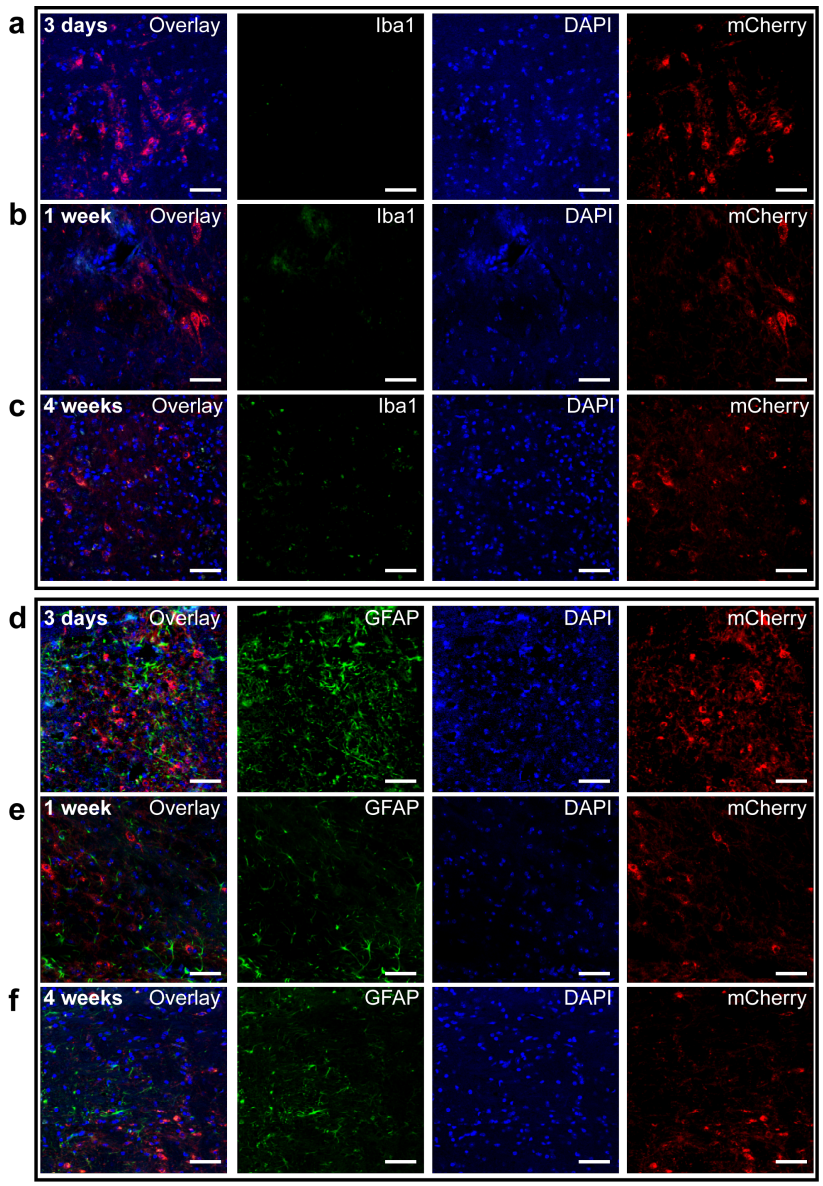

Fig. S19. Biocompatibility assessment of the magnetoliposome injections. Confocal images of (**a-c**) activated microglia (Iba1) and (**d-f**) astrocytes (GFAP) of the tissue around magnetoliposomes in a mouse VTA expressing *hsyn::hM3D(Gq)-mCherry*. All the injection procedures are identical to those used for the CNO-loaded magnetoliposomes in the FST assay. Mouse brain slices were prepared 3 days (**a**, **d**), 1 week (**b**, **e**) and 4 weeks (**c**, **f**) following magnetoliposomes injection. The experiment was repeated three times independently with similar results. Scale bar: 50 μm.

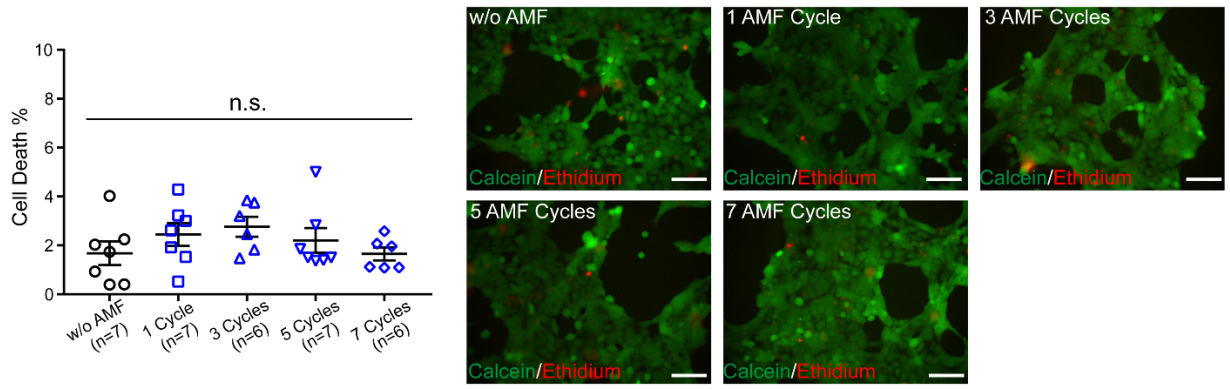

Fig. S20 Cytotoxicity assessment of the chemomagnetic modulation. HEK293 cell cultures were stained with calcein-AM (green) to indicate living cells and ethidium homodimer-1 (red) to indicate dead cells that lost plasma membrane integrity. Cell cultures were incubated with CNO-loaded magnetoliposomes and then stimulated with a series of AMF cycles. All groups show no significant cell death as confirmed by one-way ANOVA and Turkey's multiple comparisons test ($F_{4,\,28}$ = 1.129, n.s. P≥0.05, w/o AMF vs. 1 cycle p=0.72, w/o AMF vs. 3 cycles p=0.45, w/o AMF vs. 5 cycles p=0.91, w/o AMF vs. 7 cycles p>0.99, 1 cycle vs. 3 cycles p=0.99, 1 cycle vs. 5 cycles p>0.99, 1 cycle vs. 7 cycles p=0.73, 3 cycles vs. 5 cycles p=0.91, 3 cycles vs. 7 cycles p=0.46, 5 cycles vs. 7 cycles p=0.90). Solid lines: mean±s.e.m., AMF conditions: H_0 =45±2 mT, f = 164 kHz, 40 s ON epochs followed by 40 s OFF rest periods. n is the number of independent experiments.

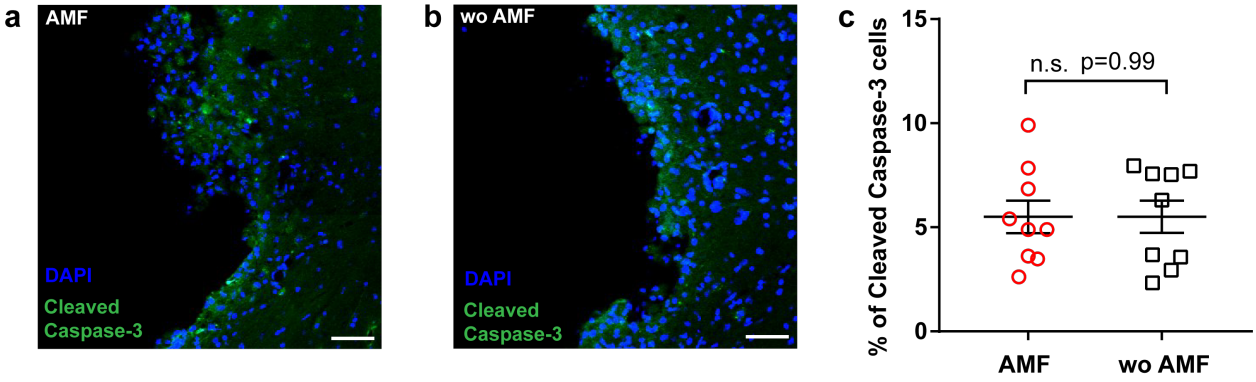

Fig. S21 Cell damage assessment of AMF stimulation. a-b, Confocal images of the interface between the magnetoliposome injection cites and the brain tissue with and without AMF stimulation. The experiment was repeated three times independently with similar results. **c,** The percentages of Cleaved Caspase-3 positive cells among DAPI-labelled cells in each group. No significant difference (n.s. p≥0.05) was found between the groups exposed and not exposed to AMF. Error bars indicate mean ± s.e.m., n=3 mice, three interface sites are used for analysis of each mouse, unpaired t-test, two tailed p-value. AMF conditions: H_0=45±2 mT, f=150 kHz, 40 s.

Table S1 Equation and parameters used in the Abaqus model of CNO diffusion

Parameter	Unit	Notation	Value	Reference
Diffusion coefficient in tissue	m^2/s	D_{tissue}	1.58×10^{-10}	7-9
Water diffusion coefficient	m^2/s	D_{tissue}	4.0×10^{-10}	10
Source concentration	mM	C_{source}	14.6	N/A

Mass diffusion described by Fick's law[11]:

$$\mathrm{J} = -\mathrm{D} \cdot \frac{\partial c}{\partial x} \qquad \text{Equation (1)}$$

J: the flux of concentration of the diffusing phase
c: the mass concentration of the diffusing material
D: the diffusivity
x: the distance from the diffusion source

Supplementary references:

1 Chen, R. *et al.* High-performance ferrite nanoparticles through nonaqueous redox phase tuning. *Nano Lett.* **16**, 1345-1351 (2016).
2 Romero, G., Christiansen, M. G., Stocche Barbosa, L., Garcia, F. & Anikeeva, P. Localized Excitation of Neural Activity via Rapid Magnetothermal Drug Release. *Adv. Funct. Mater.* **26**, 6471-6478 (2016).
3 Christiansen, M. G., Howe, C. M., Bono, D. C., Perreault, D. J. & Anikeeva, P. Practical methods for generating alternating magnetic fields for biomedical research. *Rev. Sci. Instrum.* **88**, 084301 (2017).
4 Chen, R., Romero, G., Christiansen, M. G., Mohr, A. & Anikeeva, P. Wireless magnetothermal deep brain stimulation. *Science* **347**, 1477-1480 (2015).
5 Takahashi, S., Shibata, M. & Fukuuchi, Y. Effects of increased extracellular potassium on influx of sodium ions in cultured rat astroglia and neurons. *Dev. Brain Res.* **104**, 111-117 (1997).
6 Baylor, D. & Nicholls, J. Changes in extracellular potassium concentration produced by neuronal activity in the central nervous system of the leech. *J. Physiol.* **203**, 555-569 (1969).
7 Zhan, W. & Xu, X. Y. A mathematical model for thermosensitive liposomal delivery of doxorubicin to solid tumour. *J. Drug Deliv.* **2013** (2013).
8 Goh, Y.-M. F., Kong, H. L. & Wang, C.-H. Simulation of the delivery of doxorubicin to hepatoma. *Pharm. Res.* **18**, 761-770 (2001).
9 Eikenberry, S. A tumor cord model for doxorubicin delivery and dose optimization in solid tumors. *Theor. Biol. Med. Model.* **6**, 16 (2009).
10 Zhao, S., Zhao, H., Zhang, X., Li, Y. & Du, Y. Off-the-shelf microsponge arrays for facile and efficient construction of miniaturized 3D cellular microenvironments for versatile cell-based assays. *Lab Chip* **13**, 2350-2358 (2013).
11 Fick, A. Ueber diffusion. *Annalen der Physik* **170**, 59-86 (1855).